THE JOURNAL OF PHYSICAL CHEMISTRY C

Article

pubs.acs.org/JPCC

Emergence of Novel Polynitrogen Molecule-like Species, Covalent Chains, and Layers in Magnesium−Nitrogen Mg_xN_y Phases under High Pressure

Shuyin Yu,[†,‡] Bowen Huang,[§] Qingfeng Zeng,[†,‡] Artem R. Oganov,[∥,‡,⊥,#] Litong Zhang,[†] and Gilles Frapper*[,§]

[†]Science and Technology on Thermostructural Composite Materials Laboratory, School of Materials Science and Engineering, Northwestern Polytechnical University, Xi'an, Shaanxi 710072, China

[‡]International Center for Materials Discovery, School of Materials Science and Engineering, Northwestern Polytechnical University, Xi'an, Shaanxi 710072, China

[§]IC2MP UMR 7285, Université de Poitiers - CNRS, 4, rue Michel Brunet TSA 51106−86073 Cedex 9 Poitiers, France

[∥]Skolkovo Institute of Science and Technology, 3 Nobel Street, Moscow 143026, Russia

[⊥]Department of Geosciences, Center for Materials by Design, and Institute for Advanced Computational Science, State University of New York, Stony Brook, New York 11794-2100, United States

[#]Moscow Institute of Physics and Technology, Dolgoprudny, Moscow Region 141700, Russia

Supporting Information

ABSTRACT: Stable structures and stoichiometries of binary Mg−N compounds are explored at pressures from ambient up to 300 GPa using ab initio evolutionary simulations. In addition to Mg_3N_2, we identified five nitrogen-rich compositions (MgN_4, MgN_3, MgN_2, Mg_2N_3, and Mg_5N_7) and three magnesium-rich ones (Mg_5N_3, Mg_4N_3 and Mg_5N_4), which have stability fields on the phase diagram. These compounds have peculiar structural features, such as N_2 dumbbells, bent N_3 units, planar SO_3-like $N(N)_3$ units, N_6 six-membered rings, 1D polythiazyl S_2N_2-like nitrogen chains, and 2D polymeric nitrogen nets. The dimensionality of the nitrogen network decreases as magnesium content increases; magnesium atoms act as a scissor by transferring valence electrons to the antibonding states of nitrogen sublattice. In this context, pressure acts as a bonding glue in the nitrogen sublattice, enabling the emergence of polynitrogen molecule-like species and nets. In general, Zintl−Klemm concept and molecular orbital analysis proved useful for rationalizing the structural, bonding and electronic properties encountered in the covalent nitrogen-based units. Interestingly, covalent six-membered N_6^{4-} rings containing $P\bar{1}$ (I) MgN_3 phase is recoverable at atmospheric pressure. Moreover, ab initio molecular dynamics analysis reveals the polymeric covalent nitrogen network, poly-N_4^{2-}, encountered in the high-pressure *Cmmm* MgN_4 phase can be preserved at ambient conditions. Thus, quenchable MgN_4, stable at pressures above 13 GPa, shows that high energy-density materials based on polymeric nitrogen can be achievable at reduced pressures. The high-pressure phase $P\bar{1}$ (I) MgN_3 with covalent N_6 rings is the most promising HEDM candidate with an energy density of 2.87 kJ·g^{-1}, followed by $P\bar{1}$ MgN_4 (2.08 kJ·g^{-1}).

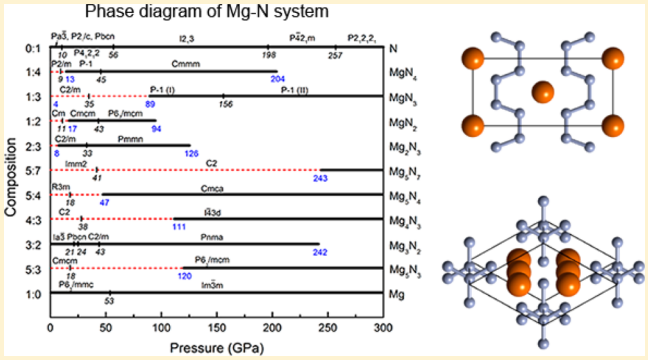

1. INTRODUCTION

The discovery and synthesis of environmentally harmless high energy-density materials (HEDMs) is now more important than at any time in the past. Among the myriad HEDMs, polynitrogen compounds are of significant interest due to their particularly high specific energy, high enthalpy of formation among other features.[1−3] Moreover, polynitrogen compounds represent a clean energy source as the final product is environmentally harmless nitrogen gas. The high energy content of polynitrogen compounds stems from the remarkable difference in the average bond energy between N−N single/double bonds (160 and 418 kJ/mol) and triple bonds (954 kJ/mol) in the N_2 molecule.[4] Transformation of polynitrogen compounds to N_2 gas is accompanied by a very large energy release. Though numerous theoretical studies predicted that polymeric phases of pure nitrogen might be stable,[5,6] it was not until 2004 that the cubic gauche structure (cg-N) was experimentally synthesized at high pressure and high temper-

Received: January 16, 2017
Revised: April 21, 2017
Published: April 21, 2017

DOI: 10.1021/acs.jpcc.7b00474
J. Phys. Chem. C 2017, 121, 11037−11046

ature (110 GPa, 2000 K).[7] This single-bonded nitrogen material possesses the unique property that its estimated energy capacity is more than five times than that of the most powerful non-nuclear energetic materials.[8]

However, Eremets et al. found that at room temperature cg-N is metastable at pressures above 42 GPa, below which it transforms to a molecular phase under weak laser illumination. One effective approach to stabilize such polymeric nitrogen phases is to form nitrogen-rich alloys with other elements; such "chemical precompression" may significantly reduce the pressure of polymerization. Inspired by elusive polymeric nitrogen, theoretical and experimental research has made considerable progress in the exploration of stable nitrogen-rich compounds, including the alkali metal azides AN_3 (A = Li, Na, K, Cs),[9−12] LiN_5,[13] N_2H,[14,15] the C−N system,[16,17] the Hf−N system,[18] the Cr−N system,[19] and the P−N system,[20] among others. However, there have been few studies focusing on the exploration of alkali earth metal nitrides. When combined with nitrogen, these highly electropositive *s*-block elements have unusual chemistry in the solid state, suggesting unexpected stoichiometries and exploitable physical properties.[21,22]

The nitride chemistry of magnesium is relatively underdeveloped compared to its analogues (Be, Ca, Sr, Ba). Only stoichiometric Mg_3N_2 has been identified, while three known crystalline forms of calcium nitrides exist at ambient conditions, namely Ca_2N, Ca_3N_2, and CaN_2.[23−25] Interestingly, Ca_2N has a layered structure, which represents a new type of electride with 2D confinement of anionic electrons.[26] Recently, Zhu et al.[27] theoretically explored the phase diagram of the Ca−N system between 0 and 100 GPa, and discovered a series of new compounds, including Ca_2N_3, CaN, CaN_3, CaN_4, and CaN_5. The predicted compounds contain a rich variety of polynitrogen forms ranging from small molecules (N_2, N_4, N_5 and N_6) to extended nitrogen chains. For Mg_3N_2, a cubic $Ia\bar{3}$ structure (antibixbyite α-Mg_3N_2) is known at ambient conditions. The α-Mg_3N_2 form is a direct band gap semiconductor with a relatively large exciton binding energy, which can be used in visible light emitters and detectors.[28]

As a crucial thermodynamic parameter, pressure has emerged as a powerful tool to investigate the physical and chemical behaviors of materials and this has led to new and unexpected products. In the present study, we investigate the possible formation and stability of polymeric nitrogen compounds in the binary Mg−N system at high pressure. Structure searches for stable Mg−N compounds were performed using an unbiased evolutionary structure prediction algorithm[29−31] in conjunction with density-functional calculations. Then, electronic properties and chemical bonding of the identified compounds were systematically investigated, in order to explore the properties and potential applications of Mg−N compounds as high energy-density materials.

During the reviewing process, a theoretical study of the phase diagram of binary Mg−N system between 0 and 100 GPa was published by Wei et al.[18] Besides Mg_3N_2, they proposed five Mg_xN_y stoichiometries (see SI), while our variable-composition evolutionary searches have led to eight stoichiometries. Nevertheless, an original covalent nitrogen net made of six-membered N_6 rings is predicted in a high-pressure MgN_3 phase, as well as *P*−1 MgN_4 and *Pnma* Mg_3N_2 phases. Therefore, these phases complement well our extensive study of Mg−N system under high pressure (0−300 GPa), and we included these new results.

2. COMPUTATIONAL DETAILS

To identify stable ground-state structures and compositions of binary Mg−N system, a variable-composition evolutionary algorithm implemented in the USPEX code[29−31] was employed. The total number of atoms in the primitive cell was up to 30. The first generation had 100 randomly produced candidate structures; all subsequent generations contained 80 structures. Evolutionary variation operators were applied to produce new structures; 60% of the new structures were produced by heredity with the remaining structures produced by softmutation (15%), transmutation (15%), and random generation (10%).

Density-functional energy calculations and geometry optimizations were performed using the VASP package[32] with the Perdew−Burke−Ernzerhof parametrization of the generalized gradient approximation.[33] Projector-augmented wave (PAW)[34] potentials were used for magnesium and nitrogen atoms with radii of 2.0 a.u. for Mg ([Ne] core) and 1.5 a.u. for N ([He] core). A plane-wave basis set with a kinetic energy cutoff of 600 eV was employed. Uniform Γ-centered meshes with a reciprocal space resolution of $2\pi \times 0.03$ Å^{-1} were used for Brillouin zone sampling to ensure the error bars of the total energies were less than 1 meV/atom. Structure relaxations proceeded until all forces on atoms were less than 1 meV/Å, and total stress tensor deviated from target pressure by ≤0.01 GPa. Structural parameters for Mg_xN_y phases are given in the Supporting Information as Table S1.

The dynamical stability of the statically relaxed structures was established by the absence of imaginary phonon frequencies (see Figure S1), which were computed using the finite-displacement approach as implemented in the PHONOPY code.[35] Moreover, the effect of zero-point energy (ZPE) on the stability of Mg−N compounds was studied. The inclusion of ZPE only shifted moderately the fields of stability, but did not change the topology of the phase diagram, thus the following energies are non-ZPE corrected (see Table S2). The enthalpy of formation of Mg_xN_y compounds is defined as

$$\Delta H_f(Mg_xN_y) = [H(Mg_xN_y) - xH(Mg) - yH(N)]/(x + y) \quad (1)$$

where all enthalpies *H* are given at the same pressure and 0 K. Compounds located on the convex hull are thermodynamically stable against decomposition into any other binaries or the elements, while compounds above the convex hull are not stable.[36,37] The most stable forms of pure Mg and N depend on the applied pressure, i.e., the hcp, bcc structures for Mg[38] and $Pa\bar{3}$, *Pbcn*, $P2_1/c$, $P4_12_12$, $I2_13$, *Pba*2, and $I\bar{4}3m$ structures for N.[39,40]

3. RESULTS AND DISCUSSION

3.1. Phase Stability of the Mg−N System under Pressure. Stable compounds, which form the thermodynamic convex hull (Figure 1), were identified at selected pressures and their stability fields are shown in the pressure−composition phase diagram (Figure 2). It is noteworthy that our evolutionary searches successfully reproduced experimentally known Mg_3N_2 structures. Moreover, the searches revealed that Mg_3N_2 transforms from the $Ia\bar{3}$ to *Pbcn* phase at 21 GPa, to the *C*2/*m* phase at 24 GPa and to the *Pnma* phase at 43 GPa. The high-pressure *Pnma* phase has been proposed by Wei et al. based on first-principles particle swarm methodology imple-

DOI: 10.1021/acs.jpcc.7b00474
J. Phys. Chem. C 2017, 121, 11037−11046

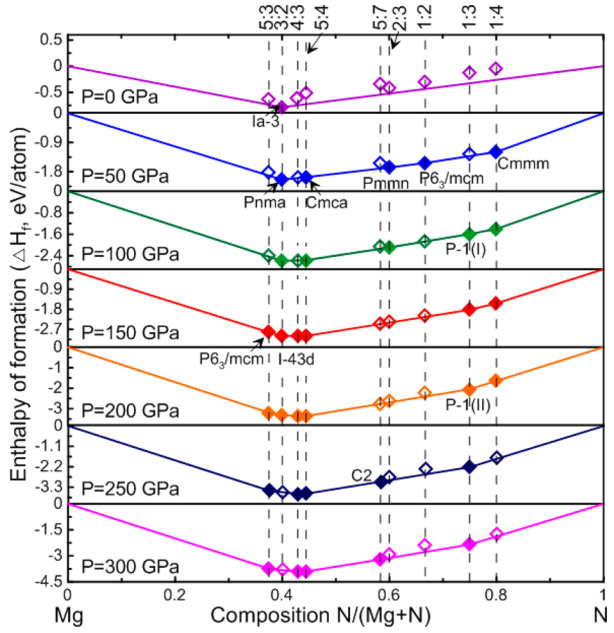

Figure 1. Convex hulls of the Mg−N system at selected pressures. Solid squares denote stable structures, while empty ones represent metastable structures.

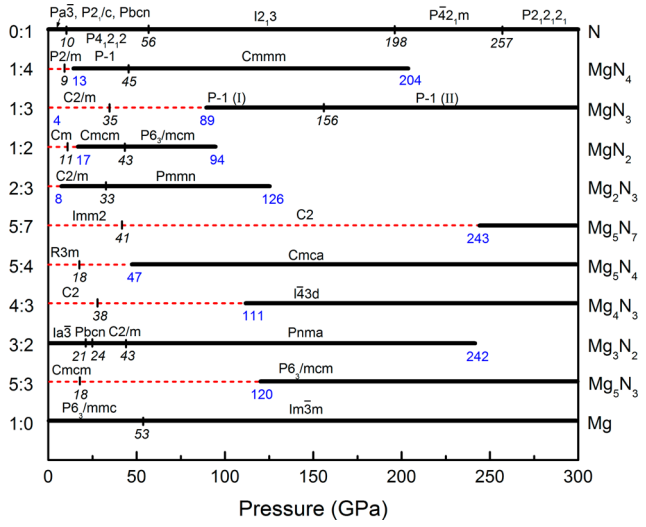

Figure 2. Pressure−composition phase diagram of Mg−N system from 0 to 300 GPa. The stable phases are indicated by bold lines and metastable phases are depicted by thin dashed lines. The blue numbers represent compound stability ranges, while black italic numbers denote phase transition pressures.

mented in CALYPSO code.[36] Besides Mg_3N_2, eight hitherto unknown stoichiometries emerged to be stable under pressure, including five N-rich stoichiometries, namely, Mg_5N_7, Mg_2N_3, MgN_2, MgN_3, and MgN_4, and three Mg-rich compositions, Mg_5N_3, Mg_4N_3, and Mg_5N_4. As shown in Figure 2, Mg_3N_2, Mg_2N_3, MgN_2, MgN_3, and MgN_4 undergo a series of phase transitions in their stability domains, while other stoichiometries only possess a single phase.

According to the structural arrangement and dimensionality of the covalent nitrogen network, the great variety of crystal structures was classified into four different categories (see Table 1): structures with (1) 1D infinite nitrogen chains (MgN_4); (2) 2D covalent nitrogen layers alternating with magnesium sheets (MgN_3); (3) encapsulated molecule-like covalent anionic units such as N_2 dumbbells, bent triatomic N_3 units and planar $N(N)_3$ motifs, as found in Mg_5N_4, Mg_5N_7, Mg_2N_3, or MgN_2; and (4) isolated nitrogen atoms, as found in Mg_5N_3, Mg_3N_2, Mg_4N_3, and Mg_5N_4. This structural classification can be applied to other alkali and alkali earth nitride A_xN_y compounds, such as N_2 dumbbells,[41,42] linear N_3 units,[41,43] five-membered N_5 rings,[13,41] cyclic N_6 rings,[27,41,44] and 1D linear N_x.[26,27,45] An up-to-date list of synthesized and predicted A_xN_y compounds is presented in Table S3.

The electronic and geometric structures of the Mg_xN_y phases were examined in order to better understand their chemical bonding. Throughout this article, electron transfer is considered to occur from electropositive magnesium atoms into the polynitrogen sublattice, thus a N_y network bears 2× valence electrons (ve) per formula unit. Except for isolated N^{3-}-based structures, covalent N−N bonds are encountered in the nitrogen sublattice. We recall the lengths of N−N bonds are roughly 1.10 Å for the triple bond, 1.25 Å for the double bond, and 1.45 Å for the single bond at ambient conditions. For calibration, the N−N single bond distance in cg-N is 1.31 Å at 200 GPa. These values were used to guide assignment of nitrogen−nitrogen bonds in order to rationalize the local structural environments using VSEPR theory and the Zintl−Klemm concept.

3.2. Compounds Containing 1D Polynitrogen Armchair Chains and Corrugated 2D Layers. *3.2.1. MgN_4.* Our evolutionary searches uncovered N-rich MgN_4 stoichiometry as a thermodynamic ground state at a pressure as low as 13 GPa, easily achievable in high-pressure synthesis. The $P\bar{1} \rightarrow Cmmm$ phase transition occurs at 45 GPa while their energy difference is as low as 0.05 eV/atom in the pressure range of 13−45 GPa. $P\bar{1}$ and $Cmmm$ structures feature infinite planar 1D armchair-shaped nitrogen chains intercalated by magnesium atoms. The structural difference of these two phases mainly comes from the poly-N_4 chain-stacking sequences. Therefore, we focus our structural and electronic analysis on the higher-symmetry $Cmmm$ phase. Its crystal structure is shown in Figure 3a. Each N atom of the poly$(N_4)_x$ chain is coordinated with two nearest Mg atoms, which are above and below the nitrogen chain plane, and each Mg atom is eight-coordinated by nearby N atoms forming an MgN_8 cube (Mg−N = 2.26 Å at 15 GPa). The shortest interchain separations are 2.77 Å along the c axis (π stacking interactions) and 2.70 Å along the b axis. The N−N separation along the chains are around 1.35 Å at 15 GPa, while the N−N−N bond angles are roughly 112°.

In the ionic picture, each Mg atom gives its two valence electrons to the N_4 building block; thus, the N_4^{2-} unit has 22 valence electrons, four σ bonding pairs, four in-plane lone pairs and six π delocalized electrons. The poly-N_4^{2-} chain is isotopological and isoelectronic to polythiazyl $-(S_2N_2)_x-$,[46] an inorganic metallic polymer. Standard application of VSEPR theory to this planar chain enabled rationalization of the structural and bonding properties of poly-N_4^{2-} chains: each nitrogen atom is bent (Figure 3b). The planarity of the whole armchair chain is the result of delocalization, but also of the strong ionic interactions between Mg^{2+} ions and poly-N_4^{2-} chains. Recall that all N−N bonds in N_4^{2-} are of nearly same length, i.e., 1.35 Å, which is longer than a double bond (1.25 Å) but shorter than a single bond (1.45 Å). This intermediate distance is consistent with the bonding picture in which six π electrons are distributed along the $-(N_4^{2-})_x-$ chain.

DOI: 10.1021/acs.jpcc.7b00474
J. Phys. Chem. C 2017, 121, 11037−11046

Table 1. Chemical Features of Stable Magnesium−Nitrogen Mg_xN_y Compounds

Phases	Space group	Stability domain (GPa)	Structure type	Nitrogen net
MgN_4	*P-1*[18]	13~45	1D armchair chains 2-coordinate N	
	Cmmm	45~204		
MgN_3	*P-1* (I)[18]	89~156	benzene-like N_6 rings	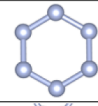
	P-1 (II)	156~300	2D layers 2- and 3-coordinate N	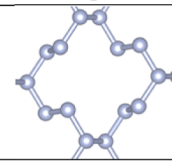
MgN_2	*Cmcm*	17~43	N_2 dumbbells	
	$P6_3/mcm$	43~94	$N(N)_3$ three-pointed stars	
Mg_2N_3	*C2/m*	8~33	isolated nuclei N_2 dumbbells	
	Pmmn	33~126	bent N_3 units	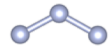
Mg_5N_7	*C2*	243~300	N_2 dumbbells bent N_3 units	
Mg_5N_4	*Cmca*	47~300	isolated nuclei N_2 dumbbells	
Mg_4N_3	*I-43d*	111~300	isolated nuclei	
Mg_3N_2	*Ia-3*	0~21	isolated nuclei	
	Pbcn	21~24	isolated nuclei	
	C2/m	24~43	isolated nuclei	
	Pnma[18]	43~242	isolated nuclei	
Mg_5N_3	$P6_3/mcm$	120~300	isolated nuclei	

To confirm this analysis from the perspective of the simplified yet useful Zintl−Klemm concept and Lewis theory, the electron localization function (ELF) was calculated. Topological analysis of ELF reveals the presence of two kinds of attractors (Figure S2). Each nitrogen atom has three valence basins: two disynaptic valence basins (N−N bonds) and one monosypnatic basin (a lone electron pair). This confirms the sp^2-like nature of the N−N bonding in the *Cmmm* structure. To assess if this poly nitrogen anionic chain is metallic like polythiazyl $-(S_2N_2)_x-$, we chose to start with the planar *cis*-N_4^{2-} molecular unit, then built the extended armchair chain. The open *cis*-N_4^{2-} unit has four π molecular orbitals (1 AO π per nitrogen atom) and six π electrons. Two bonding π_1 and π_2 and one antibonding HOMO π_3* exist and are occupied, while the highest in energy, antibonding π_4*, remains vacant. The molecular orbital diagrams are displayed in Figure 3c. When converting from the molecular planar *cis*-N_4^{2-} unit to the extended poly-N_4^{2-} system, each π orbital generates a dispersive π band in the entire Brillouin zone (Γ-X line). If no band overlap occurs, one may expect semiconductor behavior for the $-(N_4^{2-})_x-$ chain. If band overlap occurs, joint valence and conducting (π_3*, π_4*) bands exist; in this case, the armchair polynitrogen anionic chain would be a metallic conductor.

The densities of states (DOS) of *Cmmm* MgN_4 were computed, shown in Figure 3d. This phase is calculated to be metallic; the bands crossing the Fermi level are π-like, i.e., joint (π_3*, π_4*) bands with some lone pair characteristics. Note that a Peierls distortion should occur in the $-(N_4^{2-})_x-$ chain as the Fermi level crosses π bands, though the strong ionic interactions between Mg^{2+} cations and $-(N_4^{2-})_x-$ chains should prevent substantial Peierls distortion of the polymeric chain. As a result, the alternating N−N bond length differences along the covalent nitrogen chain are small, less than 0.01 Å. To conclude, MgN_4 contains planar nitrogen-based $-(N_4^{2-})_x-$ chains, and is an analogue of the inorganic $-(S_2N_2)_x-$ polythiazyl polymer. MgN_4 should behave as a highly anisotropic conductor at room temperature. The isoelectronic and isotopological polynitrogen chain was also discovered by Zhu et al.[27] in the $P4_12_12$ CaN_4 phase.

3.2.2. MgN_3. In the nitrogen-rich side of the phase diagram, the structure search also yielded the composition MgN_3 with a phase transition sequence of *C2/m* (0 GPa, isolated N_2 dummbels) → *P*−1 (I) (35 GPa, isolated N_6 rings) → *P*−1 (II) (156 GPa, covalent nitrogen layers). However, the low-pressure *C2/m* phase, $(2Mg^{2+})(3N_2)^{4-}$ appears as metastable, as it is above the convex hull. MgN_3 presents only two thermodynamically stable phases, *P*−1 (I) from 89 to 156 GPa

DOI: 10.1021/acs.jpcc.7b00474
J. Phys. Chem. C 2017, 121, 11037−11046

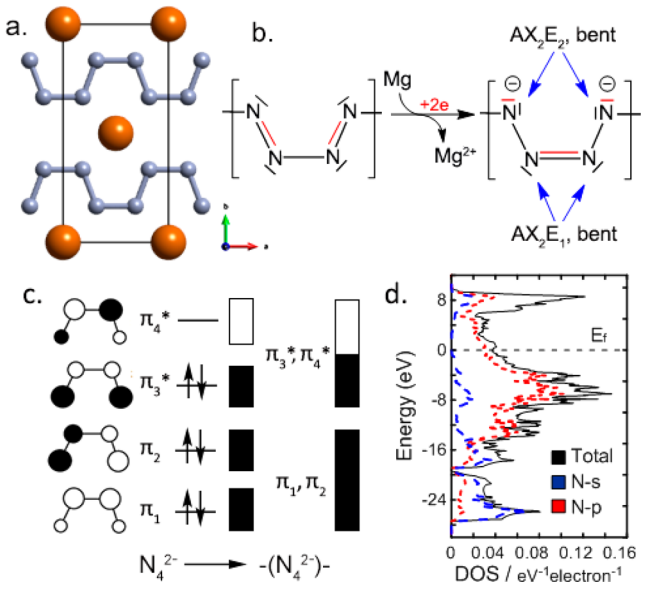

Figure 3. (a) Crystal structure of *Cmmm* MgN_4. The large orange circles represent Mg atoms, while small blue ones denote N atoms. (b) Scheme illustrating electron transfer from electropositive Mg atoms to the 1D poly$(N_4)_x$ chain and VSEPR AX_nE_m notation (A, central atom; X, ligand and *n*, its number; E, lone pairs and m its numbers; $n + m$ is the steric number). (c) Molecular orbital diagram of the open N_4^{2-} π system. The right side shows the schematic band structure of the $-(N_4^{2-})_x-$ chain without (left) and with (right) band overlap. (d) Calculated density of states of *Cmmm* MgN_4 at 100 GPa.

and *P*−1 (II) above 156 GPa. Our results are in agreement with Wei et al. ones who proposed a stable *P*−1 (I) phase above 80 GPa.[18] Moreover, from a theoretical point of view, *P*−1 (I) phase can be recovered at atmospheric pressure while high-pressure *P*−1 (II) phase can not.

In *P*−1 (I) phase, nitrogen atoms form six-membered N_6 rings as shown in Figure 4a. At 100 GPa, a chair conformation

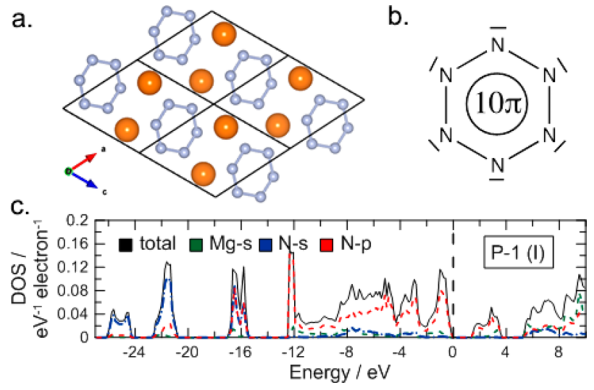

Figure 4. (a) Crystal structure of *P*−1 (I) MgN_3. (b) Lewis structure of cyclic N_6^{4-} anion. (c) Calculated density of states for *P*−1 (I) MgN_3 at 100 GPa.

is observed with a calculated dihedral angle of 150°. When pressure is released to 1 atm (the Mg−N Madelung energy and the packing forces decrease), covalent hexazine-N_6 anion remains intact and becomes planar with six nearly identical N−N bonds of 1.39 Å, which are slightly shorter than a single N−N bond (1.45 Å) but longer than a double one (1.25 Å). Formally, magnesium atoms transfer all of their valence electrons to N_6 rings, leading to N_6^{4-} unit. This 10 π-electron 6-membered ring follows the $4n + 2$ Hückel rule (aromatic), and it is isolectronic to the well-known inorganic cyclic $S_3N_3^-$ and P_6^{4-} species.[37] A molecular orbital diagram of the benzene-like N_6^{4-} anion is displayed in Figure S3. Among the six π levels of planar N_6 ring, the three bonding π molecular orbitals (MO) and the two degenerated antibonding π^* ones are fully occupied, leading to only one π−bond delocalized over the 6 nitrogen atoms. This electronic situation explains well the structural feature encoutered in N_6^{4-}, e.g., N−N bonds slightly stronger than usual single N−N bond. An energy gap separates the degenerate occupied π_4^* and π_5^* MO (top of the valence band) and the empty π_6^* MO (bottom of the conduction band); MgN_3 is a semiconductor (see Figure 4c).

As mentioned previously, *P*−1 (I) has no imaginary phonons from its range of stability down to $P = 1$ atm, and presents persistent six-membered N_6^{4-} ring motif. If the barrier to decomposition to elements or others Mg_xN_y phases can protect *P*−1 (I) phase, then perhaps this original aromatic hexazine-N_6 dianion could be detected.

Above 156 GPa, a novel stable phase emerges on the energy surface as a static ground-state structure (space group: *P*−1). Its crystal structure is shown in Figure 5a. This high-pressure

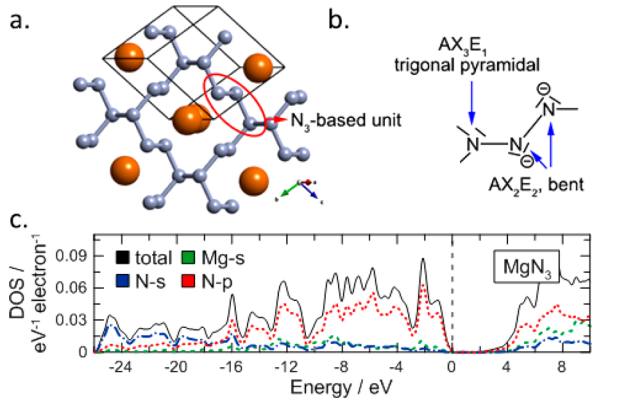

Figure 5. (a) Crystal structure of *P*−1 (II) MgN_3. (b) Lewis structure of the N_3-based unit N_3^{2-} with VSEPR AX_nE_m notation (A, central atom; X, ligand and *n*, its number; E, lone pairs and m its numbers; $n + m$ is the steric number). (c) Calculated density of states at 200 GPa.

P−1 (II) phase contains extended 2D nitrogen sheets separated by isolated magnesium atoms. The 2D nitrogen sublattice is closely related to the orthorhombic layered black phosphorus structure (α-P, space group: *Cmca*), which is composed of condensed P_6 rings in a chair conformation and can be derived from α-P by removing one-quarter of the phosphorus atoms (Figure S4). This covalent nitrogen sublattice is also isostructural to the network found in the isoelectronic α-SrP_3 phase.[47]

In MgN_3, each nitrogen slab is based on puckered 14-membered nitrogen ring which contains four N_3 units with two different types of nitrogen (>N−N−N−). This N_3 building block is illustrated in Figure 5b. One atom has a trigonal pyramidal conformation and the others have a bent conformation with N−N separations in the range of 1.33−1.40 Å at 200 GPa (single bond character). The N−N−N bond angles vary from 88 to 113°, within the allowable range for sp^3 hybrid bond angles. The geometric structure of the > N−N−N− unit is well explained by VSEPR theory if one assigns a formal charge of −1 to each two-coordinated nitrogen atom (Figure 5b). Thus, MgN_3 belongs to the family of Zintl phases;

DOI: 10.1021/acs.jpcc.7b00474
J. Phys. Chem. C 2017, 121, 11037−11046

all of the nitrogen atoms can fulfill the octet rule and all valence electrons are in localized states; therefore, $P\bar{1}$ MgN_3 should be an insulator or a semiconductor with a band gap between the occupied bonding and nonbonding nitrogen-based orbitals and the vacant orbitals, i.e. the antibonding nitrogen-based levels and Mg(3*s*) levels. Based on the computed DOS, MgN_3 is a semiconductor with a DFT band gap of 2.2 eV at 200 GPa (Figure 5c). Note that the band gap increases to 3.3 eV when a screened hybrid functional HSE06 is used (Figure S5).

3.3. Compounds Containing Molecule-like Covalent Anionic Units. *3.3.1. MgN_2.* As shown in Figure 2, MgN_2 is stable between 17 and 94 GPa, and has two phases, with the transition *Cmcm* to $P6_3/mcm$ pressure of 43 GPa. The *Cmcm* structure consists of N_2 dimers sitting in the channels of a 3D magnesium network (Figure 6a). At 40 GPa, the N−N distance

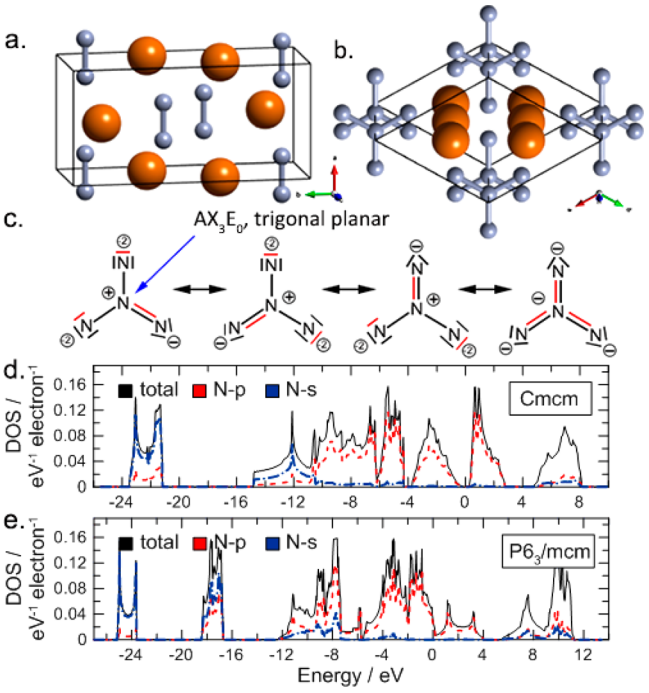

Figure 6. (a, b) Crystal structures of *Cmcm* and $P6_3/mcm$ MgN_2. (c) Resonant Lewis structure of the planar $N(N)_3^{4-}$ unit with VSEPR notation. (d, e) Calculated density of states for the *Cmcm* phase at 40 GPa and $P6_3/mcm$ phase at 100 GPa.

is 1.25 Å, indicating N−N double bond character. According to the Zintl−Klemm concept, MgN_2 can be described as $Mg^{2+}N_2^{2-}$. Thus, diazenide N_2^{2-} has 12 valence electrons and its electronic ground-state configuration is $1\sigma_g^2 2\sigma_u^{*2} 1\pi_u^4 2\sigma_g^2 1\pi_g^{*2}$ (Figure S6). The N_2^{2-} dumbbell possesses a bond order of 2 and the N_2^{2-} unit is a solid-state equivalent of molecular triplet O_2. As shown in the calculated DOS (Figure 6d), $1\pi_g^*$ degeneracy is broken by the static electric field created by the surrounding Mg^{2+} ions. Therefore, a small gap is created between these two antibonding HOMO−LUMO $1\pi_g^*$ levels. *Cmcm* MgN_2 is a very narrow-gap semiconductor with a band gap of 0.25 eV at 40 GPa.

Above 43 GPa, the most stable MgN_2 phase has $P6_3/mcm$ symmetry; its structure is displayed in Figure 6b and can be thought of as being composed of isolated flat triangular $N(N)_3$ units sitting in hexagonal prisms formed by 12 Mg atoms. Each planar $N(N)_3$ moiety possesses D_{3h} symmetry with N−N bond lengths of 1.28 Å at 100 GPa. Based on our current knowledge, this three-pointed star motif is proposed here and in our recent work[19] for the first time in nitrides. The metal atoms bear a +2 positive charge, whereas each polynitrogen anion has a −4 negative charge, i.e., $N(N)_3^{4-}$; thus, the $N(N)_3^{4-}$ unit has 24 valence electrons (Figure 6c) and is an all-nitrogen analogue that is isoelectronic to the carbonate CO_3^{2-} and nitrate NO_3^- anions, and neutral gaseous sulfur trioxide SO_3. At 100 GPa, band gap closure appears as pressure becomes higher due to increased $\pi-\pi$ interactions between stacked $N(N)_3$ units (Figure 6e).

3.3.2. Mg_2N_3. Mg_2N_3 becomes thermodynamically stable between 8 and 126 GPa. A $C2/m \rightarrow Pmmn$ phase transition occurs at 33 GPa. In the $C2/m$ structure, we can clearly see layering at ambient pressure as displayed in Figure 6a. Each Mg_2N slab is built from 2D hexagonal double layers of Mg atoms, with nitrogen atoms centering Mg_6 octahedra within the layers. These slabs are isostructural to layered subnitride A_2N slabs (A = Ca, Sr, Ba; *anti*-$CdCl_2$-type structure, space group $R\bar{3}m$),[48] with N_2 dimers filling the voids between Mg_2N layers. Formally, $C2/m$ Mg_2N_3 can be described as $(Mg^{2+})_2(N^{3-})(N_2^-)$. As expected from simple molecular orbital consideration (Figure S6), an elongated triple N−N bond is expected in N_2^- dimer as the antibonding $1\pi_g^*$ level of this 11-electron diatomic unit is formally singly occupied. This is what happens in $C2/m$ Mg_2N_3; a N−N distance of 1.18 Å is computed at 1 atm, a value setting between a triple bond (1.10 Å) and a double bond (1.25 Å). To summarize, $C2/m$ structure may be viewed as a A_2N-type layered Mg_2N structure with intercalated N_2 dummbells.

Let us now focus on the high-pressure *Pmmn* structure of Mg_2N_3. Its crystal structure is shown in Figure 7b. To the best of our knowledge, this is the first binary nitride of an *s*-block element in which a bent triatomic N_3 motif is observed rather than the classical linear motif, i.e., azide N_3^- with 16 valence

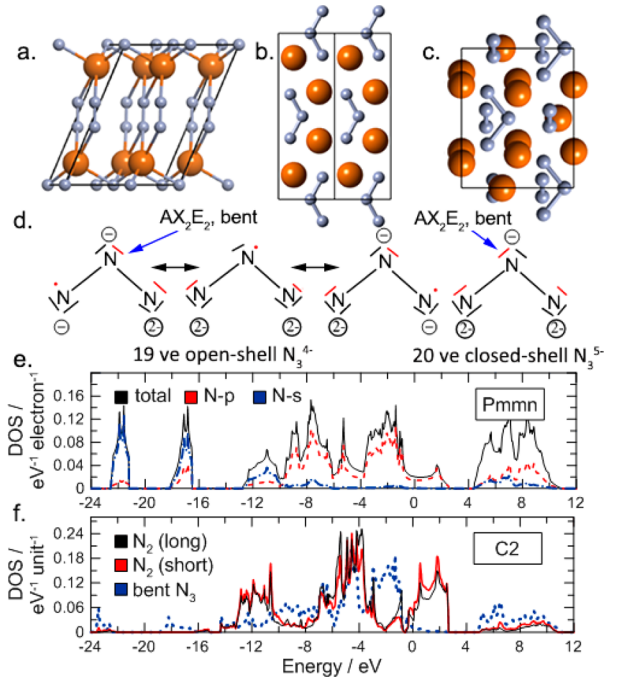

Figure 7. (a−c) Crystal structures of $C2/m$ and *Pmmn* Mg_2N_3, and $C2$ Mg_5N_7. (d) Lewis structures of the bent 19 ve N_3^{4-} and 20 ve N_3^{5-} anions. Delocalized π electrons or pairs are shown in red. (e, f) Calculated density of states for *Pmmn* Mg_2N_3 at 50 GPa and $C2$ Mg_5N_7 at 250 GPa.

DOI: 10.1021/acs.jpcc.7b00474
J. Phys. Chem. C 2017, 121, 11037−11046

electrons. Note that this unprecedented discrete bent triatomic N_3 species is also encountered in Mg_5N_7 (Figure 7c). The calculated N−N interatomic distances for *Pmmn* Mg_2N_3 at 50 GPa are 1.37 Å with a N−N−N bond angle of 122°. The electropositive Mg atoms can provide four electrons per formula unit, thus forming a 19 valence electron species N_3^{4-}, which is isoelectronic to molecular open-shell O−Cl−O. Starting from the well-known azide N_3^-, the three extra electrons found in N_3^{4-} would occupy the degenerate antibonding π_u^* orbitals of a linear triatomic species (Figure 8). This situation leads to Jahn−Teller instability. The two π_u^*

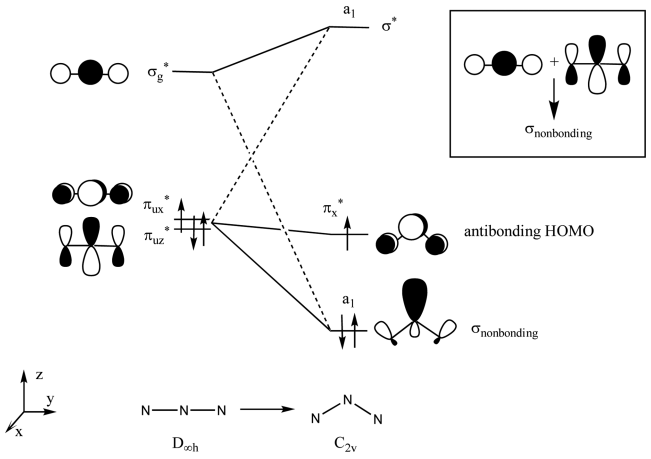

Figure 8. Simplified correlation diagram of the main orbitals of the linear and bent N_3^{4-} molecular system.

levels split by distortion to an angular structure due to *s-p* orbital mixing. The two a_1 molecular orbitals can mix in bent N_3 (ex-π_{uz}^* and σ^*), then the π_{uz}^* level (antibonding at 180°) is strongly stabilized and becomes nonbonding (formally, a lone pair orbital localized on the central atom, see the Lewis structures in Figure 7d).[49]

For an electron count of 19 valence electrons in N_3^{4-}, a radical species is identified; its HOMO is singly occupied and π antibonding in character, as depicted in Figure 8. Orbital interaction analysis explains why the main group, specifically polynitrogen triatomic species with 17 to 20 valence electrons would be bent[50] (O−N−O, 17 ve, 134°; O−N−O, 18 ve, 118°; O−S−O, 18 ve, 119°; O−Cl−O, 19 ve, 117°). This is consistent with the VSEPR theory, as the 16 ve AB_2 systems have steric number 2, giving linear molecule geometry, while the 17−20 ve AB_2 systems have steric number 3 or 4, which will give bent molecule geometry with one or two lone pairs on the central atom. The calculated electronic DOS also corroborates our findings (Figure 7e): the Fermi level crosses a region mainly based on nitrogen π antibonding states, i.e., the π_x^* of molecule-like N_3^{4-}. Half of the π_x^* band is filled, thus Mg_2N_3 is metallic.

3.3.3. Mg_5N_7. This 5:7 composition is thermodynamically stable at very high pressures (above 243 GPa) and adopts the *C*2 structure (Figure 7c). N_2 dumbbells and bent N_3 units in the nitrogen sublattice are embedded in the magnesium framework. First, we focused on bonding analysis of the bent N_3 unit. In Mg_5N_7, C_{2v} N_3 has a N−N distance of 1.36 Å and bond angle of 103° at 250 GPa. Note this N−N bond length is larger than in Mg_2N_3 (1.28 Å at 250 GPa), indicating a bond order of 1. Therefore, one may assign a formal charge of −5 to the N_3 group, leading to the 20 ve triatomic species isoelectronic to bent closed-shell Cl−O−Cl. This bent geometry for N_3^{5-} conforms to the VSEPR prediction: AX_2E_2 deriving from a tetrahedron (Figure 7d). Molecular orbital analysis of linear and bent triatomic N_3 species revealed the antibonding π_x^* level (HOMO) is occupied by two electrons in N_3^{5-}; thus, the associated band would be filled (see the Walsh diagram in Figure 8).

Besides bent N_3 units, two nonequivalent N_2 dumbbells are observed in Mg_5N_7. The shortest interatomic N−N distance is 1.25 Å at 250 GPa, indicating a double bond character, thus a formal charge of −2 may be attributed. The other nonequivalent N_2 dimer has an elongated bond length of 1.32 Å, between that of single (1.36 Å) and double (1.25 Å) bonds. Thus, one may attribute a formal charge of −3 to this dimer, which is isoelectronic to the superoxide O_2^- species encountered in the known from experiment paramagnetic KO_2 salt (O−O distance of 1.28 Å).[51] To summarize, open-shell N_2^{2-}, N_2^{3-} and diamagnetic bent N_3^{5-} species are encountered in Mg_5N_7, and these anions are stabilized via ionic interactions with Mg^{2+} cations. Mg_5N_7 may be viewed as the formal ionic limit formula $(Mg^{2+})_5(N_3)^{5-}(N_2)^{3-}(N_2)^{2-}$. As the highest occupied molecular orbital, i.e., the degenerate antibonding π^* levels of N_2^{2-} and N_2^{3-} are partially occupied by two and three electrons, respectively, one may expect that Mg_5N_7 is a metal. Indeed, this compound is metallic in character according to the DOS calculations (Figure 7f).

3.3.4. Mg_5N_4. This 5:4 composition is the first member of the Mg-rich family of stable high-pressure Mg_xN_y phases that is stable above 47 GPa. In this structure (Figure S7), magnesium atoms lie in the center of a slightly compressed octahedron formed by nitrogen atoms, while isolated nitrogen atoms lie in a distorted pentagonal bipyramid. This structure has N_2 dumbbells, with N−N distances equal to 1.44, 1.50, and 1.63 Å at 300, 200, and 50 GPa, respectively, indicative of a weakened single bond in the N_2 dimer. This behavior is more easily understood when one looks at the valence electron concentration (VEC = 7.66). A VEC close to 8 (octet rule) or higher leads to phases with isolated nitrogen atoms (Table S3). Mg_5N_4 sits at the border between phases with covalent molecule-like species and isolated N^{3-} particles. To explain the bonding mode in Mg_5N_4, this compound could be described as $(Mg^{2+})_5(N^{3-})_2(N_2)^{4-}$. With a charge of −4 per N_2 unit, the two antibonding π_g^* orbitals of N_2^{4-} are filled (Figure S6). Thus, a bond order of one is expected in N_2^{4-}, a 14 ve species isoelectronic to F_2. As magnesium completely transfers its valence electrons to the nitrogen framework, and if the N^{3-} and N_2^{4-} units follow the octet rule, this compound is expected to be an insulator or a semiconductor, in perfect agreement with the DOS calculation. A gap separates the valence and conduction bands (Figure S7), in perfect agreement with Zintl−Klemm concept.

3.4. Compounds Containing Only Isolated Nitrogen Atoms. Besides Mg_3N_2, two new compounds, Mg_5N_3 and Mg_4N_3, feature isolated nitrogen atoms. They occupy cavities inside magnesium sublattice, as depicted in Figure S7. These compounds have VEC values ranging from 7.66 to 8.33 (close to 8, octet rule), in which isolated N^{3-} anions are found. With VEC values of 7.66 and 8.33, one extra hole h^+ or electron e^- is expected over the whole structure. Thus, *p*- and *n*-type materials are predicted for the Mg_4N_3 and Mg_5N_3 phases, respectively.

Mg_5N_3 adopts a hexagonal Mn_5Si_3-type structure with the space group $P6_3/mcm$[52] and is stable above 120 GPa. This

DOI: 10.1021/acs.jpcc.7b00474
J. Phys. Chem. C 2017, 121, 11037−11046

structure consists of infinite chains of empty face-sharing Mg_6-antiprisms and isolated atoms. The formula Mg_5N_3 can be rationalized as $(Mg^{2+})_5$ $(N^{3-})_3$ $(1e^-)$. With respect to this "extra" electron, a small half-filled band composed mostly of Mg−Mg bonding is found centered on the Fermi level, as shown in Figure S7. Thus, Mg_5N_3 has a metallic behavior. Note that many Mn_5Si_3-type A_5B_3 phases well known to bind diverse atoms in the interstitial cavities within a chain of face-sharing trigonal antiprisms formed by A atoms. In Mg_5N_3, these interstitial sites are empty. We predict this Mg−Mg bonding will disappear due to insertion of hydrogen or fluorine, as observed in Ca_5Bi_3H.[53]

Mg_4N_3 crystallizes in an *anti*-Th_3P_4 type structure with the space group $I\bar{4}3d$, and becomes stable near 111 GPa. In this structural arrangement, the nitrogen atoms are eight-coordinated by magnesium atoms, while Mg atoms are octahedrally coordinated by nitrogens. A recent study also suggested an isoelectronic analogue of Mg_4N_3, the hypothetical Ca_4N_3, adopts this complex structure.[54] Such alkali earth metal nitrides can be described as Zintl phases, where magnesium atoms donate their two valence electrons to the nitrogen atoms to form closed-shell configurations. The formula of Mg_4N_3 can be written using the ionic limit $(Mg^{2+})_4(N^{3-})_3(1h^+)$ with electroneutrality being achieved by the presence of one extra hole h^+, leading to a *p*-type conductor. Therefore, from this simple electron count, the N-2p levels are not expected to be fully occupied; this was confirmed by analysis of the DOS plot (Figure S7) in which the Fermi level crossed the top of the N-2p bands, reflecting the metallicity of this high-pressure $I\bar{4}3d$ Mg_4N_3 phase.

3.5. Quenchable High-Pressure MgN_4? A Route towards High Energy-Density Materials. To further confirm the stability of the polymeric chain found in high-pressure *Cmmm* MgN_4 phase after pressure release, its associated phonon spectrum was calculated at 1 atm. After relaxation, the extended 1D nitrogen net remained intact. Moreover, the absence of any imaginary modes throughout the entire 3D reciprocal space indicates this *Cmmm* poly-N_4 containing phase is dynamically stable at 1 atm and 0 K. However, its enthalpy is 0.191 eV/atom above the lowest metastable MgN_4 phase at 1 atm, i.e., $P2/m$, which contains two isolated N_2 molecular units per formula unit. If the barrier of transformation to $P2/m$ (or decomposition to elements or other Mg_xN_y compounds) can protect *Cmmm*, then perhaps it could exist at normal conditions. Therefore, to further probe the structural stability of the covalent armchair-shaped polynitrogen chains, ab initio molecular dynamic (AIMD) simulations based on DFT were performed at different temperatures based on a 3 × 2 × 4 supercell. During the entire 10 ps AIMD simulations at temperatures of 300 K, 600 and 900 K, the covalent N−N bonds in poly-N_4^{2-} nets were not broken, and only small poly-N_4^{2-} chains shifts and Mg^{2+} cations displacements were observed (Figure 9).

To illustrate the findings, the closest N−N bond lengths fluctuate from 1.25 to1.45 Å at 900 K, suggesting bond order ranges between 1 and 2 within the covalent poly-N_4^{2-} chains. The AIMD simulations clearly suggest that the nitrogen net in *Cmmm* MgN_4 maintains integrity of the infinite planar 1D armchair-shaped chains from 0 K up to 900 K with robust thermal stability and strong kinetic trapping (at least up to 900 K). Interestingly, compared to the instability of pure nitrogen polymers, this analysis reveals the encapsulated polymeric

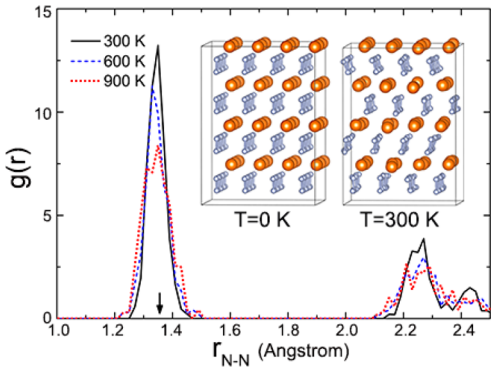

Figure 9. Radial distribution functions (RDF) for the N−N separations observed during AIMD simulations for a *Cmmm* MgN_4-based supercell at ambient pressure and temperatures of 300, 600, and 900 K. The black arrow indicates the average N−N distance in poly-N_4^{2-}.

anionic nitrogen chain in MgN_4 can be successfully preserved at ambient conditions.

Velocity of detonation (VOD), an important parameter used to evaluate the detonation properties of energetic compounds, was calculated with the Kamlet−Jacobs empirical equation[55] (calculation details are given in SI, as well as energy densities for recently predicted polynitrides and well-known HDEM in Table S4). The energy density is 2.08 $kJ{\cdot}g^{-1}$ and 2.44 $kJ{\cdot}g^{-1}$ for $P-1$ and *Cmmm*, respectively, assuming that the final products are $Mg_3N_{2(s)}$ and $N_{2(g)}$. Thus, the detonation velocity of *Cmmm* MgN_4 was found to be 11.5 km/s, which is comparable to the secondary explosive cyclotetramethylene tetranitramine $(CH_2)_4(NNO_2)_4$ HMX (VOD ∼ 9.1 km/s), but much higher than 2,4,6-trinitrotoluene-TNT explosive (VOD ∼ 6.9 km/s) and the primary explosive lead azide $Pb(N_3)_2$ (VOD ∼ 3.8 km/s).[56] Moreover, the stabilization pressure for $P-1$ MgN_4 is only 13 GPa, much lower than the pressure required to synthesize polymeric cg-N_2 (>100 GPa). High energy density, low stabilization pressure and quenchability make $P-1$ MgN_4 a candidate high energy-density material. Finally, to extend this analysis on nitrogen-rich Mg_xN_y-based HEDM compounds, we computed the energy density of all predicted Mg_xN_y phases (see Table S4). The high-pressure phase $P-1$ (I) MgN_3 with covalent N_6 rings is the most promising HEDM candidate with an energy density of 2.87 $kJ{\cdot}g^{-1}$, followed by $P-1$ MgN_4 (2.08 $kJ{\cdot}g^{-1}$), $P6_3/mcm$ MgN_2 (1.95 $kJ{\cdot}g^{-1}$) and *Pmmm* Mg_2N_3 (1.90 $kJ{\cdot}g^{-1}$).

4. CONCLUSION

In summary, we present the first complete phase diagram for the Mg−N system at pressures up to 300 GPa. High pressure may be an effective route to stable Mg nitrides with unusual stoichiometries and original, yet aesthetic, structures. Besides Mg_3N_2, eight new compositions at Mg:N ratios of 1:4, 1:3, 1:2, 2:3, 5:7, 5:3, 4:3, and 5:4 were identified. Their structures contain molecule-like covalent nitrogen units, such as N_2 dumbbells, bent N_3 motifs, planar SO_3-like $N(N_3)$ units, and benzene-like N_6 species. In addition to well-known Mg_3N_2, newly predicted Mg_5N_3 an Mg_4N_3 feature isolated N^{3-} anions. Zintl−Klemm concept, molecular orbital analysis and VSEPR theory proved useful for rationalizing the structural, bonding and electronic properties of these Mg_xN_y compounds. Notably, the dimensionality of the nitrogen network decreases as the amount of magnesium increases, with magnesium atoms acting

DOI: 10.1021/acs.jpcc.7b00474
J. Phys. Chem. C 2017, 121, 11037−11046

as a scissor by transferring their valence electrons to the antibonding states of the nitrogen sublattice. More interestingly, the polymeric nitrogen network found in MgN_4 is preserved from 0 K up to 900 K. This analysis reveals that magnesium atom plays an important role in stabilization of polymeric nitrogen networks, and that MgN_3 and MgN_4 are potential high energy-density materials. The present study contributes to understand the unusual crystal features and exploitable physical properties of nitrogen compounds under extreme conditions.

■ ASSOCIATED CONTENT

Supporting Information

The Supporting Information is available free of charge on the ACS Publications website at DOI: 10.1021/acs.jpcc.7b00474.

Calculated structural parameters, phase transitions, formation enthalpies, phonon dispersion curves, and Lewis structures of the predicted Mg_xN_ycompounds (PDF)

■ AUTHOR INFORMATION

Corresponding Author

*E-mail: gilles.frapper@univ-poitiers.fr.

ORCID

Shuyin Yu: 0000-0001-6848-1531

Gilles Frapper: 0000-0001-5177-6691

Author Contributions

The manuscript was written through contributions of all authors. All authors have given approval to the final version of the manuscript.

Notes

The authors declare no competing financial interest.

■ ACKNOWLEDGMENTS

We thank the National Natural Science Foundation of China (Nos. 51372203240 and 51332004), Foreign Talents Introduction and Academic Exchange Program (No. B08040), GDRI RFCCT CNRS (DNM-evol program), and Hubert Curien Partnerships PHC XU GUANGQI 2015 (No. 34455PE) program of the French Ministry of Foreign Affairs, Région Poitou-Charentes (France) for a Ph.D. fellowship, and the Government of the Russian Federation (No. 245 14.A12.31.0003) for financial support. We also acknowledge the High Performance Computing Centers of the NWPU (China) and Poitiers University (France), and the TGCC/Curie GENCI (France) under project n°×2016087539 for allocation of computing time.

■ REFERENCES

(1) Lauderdale, W. J.; Stanton, J. F.; Bartlett, R. J. Stability and energetics of metastable molecules: tetraazatetrahedrane (N_4), hexaazabenzene (N_6), and octaazacubane (N_8). *J. Phys. Chem.* **1992**, *96*, 1173−1178.

(2) Glukhovtsev, M. N.; Jiao, H. J.; Schleyer, P. v. R. Besides N_2, What is the most stable molecule composed only of nitrogen atoms? *Inorg. Chem.* **1996**, *35*, 7124−7133.

(3) Christe, K. O.; Dixon, D. A.; Mclemore, D.; Wilson, W. W.; Sheehy, J. A.; Boatz, J. A. On a quantitative scale for Lewis acidity and recent progress in polynitrogen chemistry. *J. Fluorine Chem.* **1999**, *101*, 151−153.

(4) Cotton, F. A.; Wilkinson, G.; Murillo, C. A.; Bochmann, M. *Advanced inorganic chemistry*; Wiley Interscience: New York, 1988.

(5) Nosé, S.; Klein, M. L. Structural transformations in solid nitrogen at high pressure. *Phys. Rev. Lett.* **1983**, *50*, 1207−1210.

(6) Mailhiot, C.; Yang, L. H.; McMahan, A. K. Polymeric nitrogen. *Phys. Rev. B: Condens. Matter Mater. Phys.* **1992**, *46*, 14419−14435.

(7) Eremets, M. I.; Gavriliuk, A. G.; Trojan, I. A.; Dzivenko, D. A.; Boehler, R. Single-bonded cubic form of nitrogen. *Nat. Mater.* **2004**, *3*, 558−563.

(8) Klapötke, T. M.; Chapman, R. D. Progress in the area of high energy density materials. *Struct. Bonding* **2015**, 1−15.

(9) Medvedev, S. A.; Trojan, I. A.; Eremets, M. I.; Palasyuk, T.; Klapötke, T. M.; Evers, J. Phase stability of lithium azide at pressures up to 60 GPa. *J. Phys.: Condens. Matter* **2009**, *21*, 659−661.

(10) Eremets, M. I.; Popov, M. Y.; Trojan, I. A.; Denisov, V. N.; Boehler, R.; Hemley, R. J. Polymerization of nitrogen in sodium azide. *J. Chem. Phys.* **2004**, *120*, 10618−10623.

(11) Ji, C.; Zheng, R.; Hou, D.; Zhu, H.; Zu, H.; Chyu, M.-C.; Ma, Y. Z. Pressure-induced phase transition in potassium azide up to 55 GPa. *J. Appl. Phys.* **2012**, *111*, 112613−112615.

(12) Hou, D. B.; Zhang, F. X.; Ji, C.; Hannon, T.; Zhu, H. Y.; Wu, J. Z.; Ma, Y. Z. Series of phase transitions in cesium azide under high pressure studied by in situ X-ray diffraction. *Phys. Rev. B: Condens. Matter Mater. Phys.* **2011**, *84*, 7615−7619.

(13) Peng, F.; Yao, Y. S.; Liu, H. Y.; Ma, Y. M. Crystalline LiN_5 predicted from first-principles as a possible high-energy material. *J. Phys. Chem. Lett.* **2015**, *6*, 2363−2366.

(14) Yin, K. T.; Wang, Y. C.; Liu, H. Y.; Peng, F.; Zhang, L. J. N_2H: a novel polymeric hydronitrogen as a high energy density material. *J. Mater. Chem. A* **2015**, *3*, 4188−4194.

(15) Goncharov, A. F.; Holtgrewe, N.; Qian, G. R.; Hu, C. H.; Oganov, A. R.; Somayazulu, M.; Stavrou, E.; Pickard, C. J.; Berlie, A.; Yen, F.; et al. Backbone N_xH compounds at high pressures. *J. Chem. Phys.* **2015**, *142*, 214308.

(16) Dong, H. F.; Oganov, A. R.; Zhu, Q.; Qian, G. R. The phase diagram and hardness of carbon nitrides. *Sci. Rep.* **2015**, *5*, 9870.

(17) Hu, A.; Zhang, F. A nitrogen-rich C_3N_{12} solid transformed from cyanuric triazide under high pressure and temperature. *J. Phys.: Condens. Matter* **2010**, *22*, 505402.

(18) Wei, S.; Li, D.; Liu, Z.; Li, X.; Tian, F.; Duan, D.; Liu, B.; Cui, T. Alkaline-earth metal (Mg) polynitrides at high pressure as possible high-energy materials. *Phys. Chem. Chem. Phys.* **2017**, *19*, 9246−9252.

(19) Kvashnin, A. G.; Oganov, A. R.; Samtsevich, A. I.; Allahyari, Z. Computational search for novel hard chromium-based materials. *J. Phys. Chem. Lett.* **2017**, *8*, 755−764.

(20) Raza, Z.; Errea, I.; Oganov, A. R.; Saitta, A. M. Novel superconducting skutterudite-type phosphorus nitride at high pressure from first-principles calculations. *Sci. Rep.* **2013**, *4*, 5889.

(21) Michalsky, R.; Avram, A. M.; Peterson, B. A.; Pfromm, P. H.; Peterson, A. A. Chemical looping of metal nitride catalysts: low-pressure ammonia synthesis for energy storage. *Chem. Sci.* **2015**, *6*, 3965−3974.

(22) Gregory, D. H. Nitride chemistry of the s-block elements. *Coord. Chem. Rev.* **2001**, *215*, 301−345.

(23) Schneider, S. B.; Frankovsky, R.; Schnick, W. Synthesis of alkaline earth diazenides $M_{AE}N_2$ (M_{AE} = Ca, Sr, Ba) by controlled thermal decomposition of azides under high pressure. *Inorg. Chem.* **2012**, *51*, 2366−73.

(24) Bradley, R. S.; Munro, D. C.; Whitfield, M. The reactivity and polymorphism of selected nitrides at high temperatures and high pressures. *J. Inorg. Nucl. Chem.* **1966**, *28*, 1803−1812.

(25) Laurent, Y.; Lang, J.; Le Bihan, M. T. Structure du nitrure de calcium α. *Acta Crystallogr., Sect. B: Struct. Crystallogr. Cryst. Chem.* **1968**, *24*, 494−499.

(26) Lee, K.; Kim, S. W.; Toda, Y.; Matsuishi, S.; Hosono, H. Dicalcium nitride as a two-dimensional electride with an anionic electron layer. *Nature* **2013**, *494*, 336−340.

(27) Zhu, S.; Peng, F.; Liu, H.; Majumdar, A.; Gao, T.; Yao, Y. Stable calcium nitrides at ambient and high pressures. *Inorg. Chem.* **2016**, *55*, 7550−7555.

DOI: 10.1021/acs.jpcc.7b00474
J. Phys. Chem. C 2017, 121, 11037−11046

(28) Uenaka, Y.; Uchino, T. Excitonic and defect-related photoluminescence in Mg_3N_2. *J. Phys. Chem. C* **2014**, *118*, 11895−11901.
(29) Oganov, A. R.; Glass, C. W. Crystal structure prediction using ab initio evolutionary techniques: principles and applications. *J. Chem. Phys.* **2006**, *124*, 244704−244715.
(30) Oganov, A. R.; Lyakhov, A. O.; Valle, M. How evolutionary crystal structure prediction works and why. *Acc. Chem. Res.* **2011**, *44*, 227−237.
(31) Lyakhov, A. O.; Oganov, A. R.; Stokes, H. T.; Zhu, Q. New developments in evolutionary structure prediction algorithm USPEX. *Comput. Phys. Commun.* **2013**, *184*, 1172−1182.
(32) Kresse, G.; Furthmüller, J. Efficient iterative schemes for ab initio total-energy calculations using a plane-wave basis set. *Phys. Rev. B: Condens. Matter Mater. Phys.* **1996**, *54*, 11169−11186.
(33) Perdew, J. P.; Burke, K.; Ernzerhof, M. Generalized gradient approximation made simple. *Phys. Rev. Lett.* **1996**, *77*, 3865−3868.
(34) Blöchl, P. E. Projector augmented-wave method. *Phys. Rev. B: Condens. Matter Mater. Phys.* **1994**, *50*, 17953−17979.
(35) Togo, A.; Oba, F.; Tanaka, I. First-principles calculations of the ferroelastic transition between rutile-type and $CaCl_2$-type SiO_2 at high pressures. *Phys. Rev. B: Condens. Matter Mater. Phys.* **2008**, *78*, 134106.
(36) Wang, Y.; Lv, J.; Zhu, Li; Ma, Y. CALYPSO: A method for crystal structure prediction. *Comput. Phys. Commun.* **2012**, *183*, 2063−2070.
(37) Allen, C. W. Inorganic rings and polymers of the p-block elements: from fundamentals to applications. *J. Am. Chem. Soc.* **2009**, *131*, 17031−17032.
(38) Li, P. F.; Gao, G. Y.; Wang, Y. C.; Ma, Y. M. Crystal structures and exotic behavior of magnesium under pressure. *J. Phys. Chem. C* **2010**, *114*, 21745−21749.
(39) Pickard, C. J.; Needs, R. J. High-pressure phases of nitrogen. *Phys. Rev. Lett.* **2009**, *102*, 125702.
(40) Wang, X.; Wang, Y.; Miao, M.; Zhong, X.; Lv, J.; Cui, T.; Li, J.; Chen, L.; Pickard, C. J.; Ma, Y. Cagelike diamondoid nitrogen at high pressures. *Phys. Rev. Lett.* **2012**, *109*, 175502.
(41) Shen, Y.; Oganov, A. R.; Qian, G.; Zhang, J.; Dong, H.; Zhu, Q.; Zhou, Z. Novel lithium-nitrogen compounds at ambient and high pressures. *Sci. Rep.* **2015**, *5*, 14204.
(42) Zhang, X. W.; Zunger, A.; Trimarchi, G. Structure prediction and targeted synthesis: A new Na_nN_2 diazenide crystalline structure. *J. Chem. Phys.* **2010**, *133*, 194504.
(43) Ramesh Babu, K.; Vaitheeswaran, G. Lattice dynamics and electronic structure of energetic solids LiN_3 and NaN_3 : A first principles study. *Chem. Phys. Lett.* **2013**, *586*, 44−50.
(44) Wang, X.; Li, J.; Botana, J.; Zhang, M.; Zhu, H.; Chen, L.; Liu, H.; Cui, T.; Miao, M. Polymerization of nitrogen in lithium azide. *J. Chem. Phys.* **2013**, *139*, 164710.
(45) Steele, B. A.; Oleynik, I. I. Sodium pentazolate: A nitrogen rich high energy density material. *Chem. Phys. Lett.* **2016**, *643*, 21−26.
(46) Mikulski, C. M.; Russo, P. J.; Saran, M. S.; Macdiarmid, A. G.; Garito, A. F.; Heeger, A. J. Synthesis and structure of metallic polymeric sulfur nitride, $(SN)_x$, and its precursor, disulfur dinitride, S_2N_2. *J. Am. Chem. Soc.* **1975**, *97*, 6358−6363.
(47) Chen, X. A.; Zhu, L. P.; Yamanaka, S. High-pressure synthesis and structural characterization of three new polyphosphides, α-SrP_3, BaP_8, and LaP_5. *J. Solid State Chem.* **2003**, *173*, 449−455.
(48) Vajenine, G. V.; Grzechnik, A.; Syassen, K.; Loa, I.; Hanfland, M.; Simon, A. Interplay of metallic and ionic bonding in layered subnitrides AE_2N (AE = Ca, Sr, or Ba) under high pressure. *C. R. Chim.* **2005**, *8*, 1897−1905.
(49) Walsh, A. D. The electronic orbitals, shapes, and spectra of polyatomic molecules. *J. Chem. Soc.* **1953**, *3*, 2266−2288.
(50) Haaland, A. *Molecules and Models: The Molecular Structures of Main Group Element Compounds*; Oxford University Press: Oxford, 2008, 304.
(51) Abrahams, S. C.; Kalnajs, J. The crystal structure of α-potassium superoxide. *Acta Crystallogr.* **1955**, *8*, 503−506.
(52) Gottschilch, M.; Gourdon, O.; Persson, J.; de la Cruz, C.; Petricek, V.; Brueckel, T. Study of the antiferromagnetism of Mn_5Si_3: an inverse magnetocaloric effect material. *J. Mater. Chem.* **2012**, *22*, 15275−15284.
(53) Corbett, J. D.; Garcia, E.; Guloy, A. M.; Hurng, W. M.; Kwon, Y.-U.; Leonescamilla, E. A. Widespread interstitial chemistry of Mn_5Si_3-type and related phases. Hidden impurities and opportunities. *Chem. Mater.* **1998**, *10*, 2824−2836.
(54) Braun, C.; Börger, S. L.; Boyko, T. D.; Miehe, G.; Ehrenberg, H.; Höhn, P.; Moewes, A.; Schnick, W. Ca_3N_2 and Mg_3N_2: unpredicted high-pressure behavior of binary nitrides. *J. Am. Chem. Soc.* **2011**, *133*, 4307−4315.
(55) Kamlet, M. J.; Ablard, J. E. Chemistry of detonations. II. buffered equilibria. *J. Chem. Phys.* **1968**, *48*, 36−42.
(56) Agrawal, P. J. *High Energy Materials: Propellants, Explosives and Pyrotechnics*; Wiley: Weinheim, 2010.

DOI: 10.1021/acs.jpcc.7b00474
J. Phys. Chem. C 2017, 121, 11037−11046